# Long-standing Optically-excited Magnetic States in ZnO Nanoparticles

Adrien Savoyant, Clément Sebastiao, Olivier Margeat

# Long-standing Optically-excited Magnetic States in ZnO Nanoparticles

**Adrien Savoyant[*,1], Clément Sebastiao[1], Olivier Margeat[3]**

[1] Aix Marseille Univ, Université de Toulon, CNRS, IM2NP, Marseille, France
[2] Aix Marseille Univ, CNRS, CINAM, Marseille, France

**Key words:** Nanoparticles, EPR, optical excitation, ZnO

[*] Corresponding author: e-mail adrien.savoyant@im2np.fr

**The spectral dependence of the light-induced magnetic states generated in zinc oxide nanoparticles by illumination during an electron paramagnetic resonance (EPR) experiment is studied for three incident light wave lengths (451, 405 and 370 nm). The minimal wave-length excitation is found to be in the visible violet region, very close to 405 nm for all of the light-induced EPR lines. This points to a close relationship between their originating centers, despite the difference in their dynamics previously revealed by saturation recovery measurements. The study of the light-induced signals decay with time (after illumination removal) and with temperature (under constant illumination) confirms the existence of two groups of lines characterized by different dynamics. The quite unusual persistence of these magnetic states after excitation removal opens promising possibilities for encoding information within semiconducting nanoparticles.**



The generation, manipulation and detection of localized quantum states with many degrees of freedom hosted in solid medium are key points for information storage and processing technologies. Embedded and confined in crystalline nano-objects, such quantum states are likely to be oriented, arranged and possibly coupled together to form the building blocks of a computing/storing system. In order to host controllable localized quantum states, semiconducting nanoparticles (NPs) are of great interest because of the rich point-defects physics which drive their remarkable properties such as electrical conductivity, luminescence, paramagnetism, etc. In these small finite systems, the surface itself is a (two-dimensional) defect which modifies the bulk properties (energy gap[1,2], phonon modes[3,4], electromagnetic response[5]), enhances the surface-related effects (catalysis[6], surface defects[7]), and gives rise to quantum confinement effects[8,9].
In this context of nano-sized semiconductors, elementary optical excitations (excitons) are likely to interact with point defects and/or with the surface discontinuity, especially in ionic polar nano-crystals such as zinc oxide (ZnO) NPs. For example, the internal electric field due to fictious surface charges at the opposite sides of the NPs (relative to the polarization axis) is susceptible to counterbalance the coulomb attraction of the photo-generated electron-hole pair. If these surface charges are not totally canceled by adsorbed molecules and/or surface reconstruction[10], a stable localized magnetic state of non-zero total angular momentum ($J \neq 0$) can be photo-generated and detected by electron paramagnetic resonance (EPR).

In a recent work[11], we have demonstrated the existence of such localized magnetic states in two kinds of ZnO NPs, reversibly induced by white-light illumination at $T = 11$ and 85 K. A photo-induced four-line structure (FLS) has been shown to arise very probably from a $J = 2$ state, subjected to a very weak axial anisotropy ($|D| = 0.27$ $\mu$eV $= 66$ MHz). Some other light-induced EPR lines have also been detected, displaying a different dynamics (slower spin-lattice relaxation) as compared to the FLS. While the origin of all these EPR lines is yet unclear, it is nevertheless conceivable to relate at least the FLS to some strongly bound exciton with high effective angular momentum $J = 2$, as predicted by $\boldsymbol{k}.\boldsymbol{p}$ theory.

However, the $J = 2$ excitonic state cannot be directly excited by light[12] (for total angular momentum conservation reason), so that local electrical interaction(s) would be required to favour this state. On the other hand, ab initio ZnO study has predicted a $J = 2$ spin-state for the doubly positive Zn vacancy ($V_{Zn}^{2+}$), arising from the four holes localized on the four oxygen dangling bonds[13]. Therefore, at this stage, additional experimental investigations of these light-induced magnetic states, especially regarding their dynamics and energetics, have to be performed in order to characterize them more precisely and to lay the foundations of a relevant model.

In this letter, we report on the spectral dependence of this magneto-optical effect, recorded by continuous wave X-band EPR on a new series of hydrothermally grown ZnO NPs of the NP1 kind[11] (almost spherical, ∼15 nm diameter) at $T = 85$ K, as well as time and temperature studies of the photo-induced signal decay. These important features directly dictate what use can be done of these magnetic states, in terms of stability/duration and minimal excitation energy. The conditions for the appearance of these light-induced magnetic states are also specified below, pointing to the importance of the NPs surface passivation/relaxation. Growth methodology (described elsewhere[14]) is the same as that for NP1[11] resulting in similar structural and morphological properties, as pointed by their almost identical EPR spectra.
In this work, we have illuminated the powder of ZnO NPs during the EPR experiment with a 405 nm (violet) laser of 20 mW power, and with two LEDs of 451 nm (blue) and 370 nm (UV) whose power reaching the sample have been equally set to 20 mW. The band width of the LEDs is 20 nm, that is about ten times that of the laser. However, the absence of substantial wave length overlapping of the different sources allows for drawing relevant conclusions. For each of these optical excitations, the microwave (MW) power has been varied from 0.40 mW to 100 mW, in order to detect from unsaturated (0.40 mW) to fully saturated (100 mW) magnetic resonance.

First, we note that the light-induced EPR lines of interest ($L_1$ to $L_6$) have not been observed in the as-grown NPs under study, just after drying in vacuum. However, after two months of storage in air, the signal has appeared with moderate intensity (recordings of Figure 1, 36 scans), and with stronger intensity four additional months later (recordings of Figure. 2-a, only 1 scan). Then, the photo-induced signal stabilizes and does not evolve anymore. As the signal/noise ratio scales with $\sqrt{N}$ ($N$, the number of scans), the signal intensity has clearly increased up to saturation during six months. This indicates that the hydrothermally grown ZnO NPs reach very slowly their equilibrium state, in which the gaseous environment certainly plays a role by passivating the NPs surface. This will be clarified in a subsequent systematic study with different storage environments.

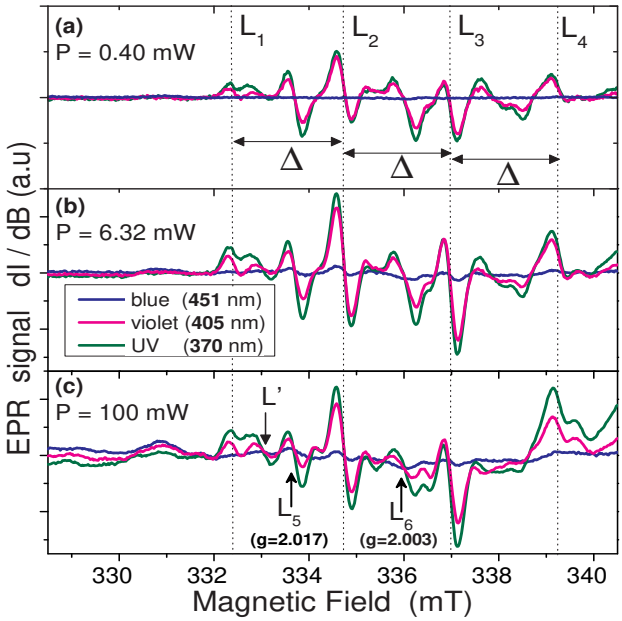


**Figure 1** (color online) EPR spectra of ZnO NPs recorded two months after growth at $T = 85$ K under 451, 405 and 370 nm wave length illumination normalized at 20 mW, for microwave power of (a) 0.40 mW, (b) 6.32 mW and (c) 100 mW and frequency of $\nu = 9.4196$ GHz . All spectra are accumulated 36 times.

In figure 1, the typical EPR spectra recorded two months after growth are shown for different MW powers and different optical excitations. In the absence of optical excitation, no lines are detected at all. These spectra mainly consist of the FLS ($L_1$ to $L_4$, spaced by $\Delta = 2.2$ mT), and of two additional lines ($L_5$ and $L_6$), all previously observed. Based on spectra simulation and MW power dependence measurement, the FLS has been assigned to an effective-spin state $J = 2$, while $L_5$ and $L_6$ have been fitted by independent 1/2 spins[11]. Other additional lines $L_7$ and $L_8$ previously observed are not sufficiently resolved here to be studied, although they can be perceived around 338 mT. At higher field ($> 340$ mT), the line's wing of the core-defect signal ($g = 1.96$)[15,16] begin to be visible, not studied here. Interestingly, another line L' is detected here between $L_1$ and $L_5$, not previously observed. However, this new line is almost not visible six months after growth in the spectra of Figure 2 where the signal/noise ratio is notably increased: its intensity has not increased with time, contrary to the other lines, certainly due to a deeper location within the NPs making it insensitive to the surface relaxation/passivation.

From figure 1, it can be seen that the minimal excitation energy of all the localized magnetic states must be

very close to that corresponding to the 405 nm violet wave length (3.06 eV), whatever the MW power set. It is interesting to note that it corresponds to visible light, whereas usual photo-excitations in ZnO require UV illumination (e.g photoluminescence.) Considering a band-gap energy of 3.4 eV, the excited magnetic states thus lie approximately 340 meV below the conduction band minimum, and must then correspond to some strongly bound states.
It is to be noted that, contrary to what can be expected from the previous MW power study[11], all lines appear uniformly when increasing the excitation energy. This suggests that at least two distinct paramagnetic centers (different in their spin-lattice relaxation) are created by the same photo-excitation. If not the case, a finer spectral study would certainly reveal a slight but substantial difference in the excitation energy of the FLS and the other lines.
As expected from the difference in energy scale, microwave power has no notable influence on the excitation energy. The unsaturated spectra ($P = 0.40$ mW) are the weaker and the smoother ones, while the fully saturated spectra ($P = 100$ mW) show line deformation, some satellite lines, and baseline disturbance. The maximal intensity is obtained for the partially saturated case ($P = 6.32$ mW).

In order to record the EPR signal decay with time after optical-excitation removal, its intensity has to be large enough to allow a reasonable signal/noise ratio with only one scan (∼40 s per scan). This condition has been obtained six months after growth, when the surface equilibrium has been reached, and by operating at the optimal MW power determined above (6.32 mW). The resulting EPR spectra recorded just after the optical-excitation removal and 110 minutes later are shown in Figure 2-a. These two spectra show the striking fact that the FLS intensity has been approximately divided by two after about two hours, while the $L_5$ and $L_6$ intensities do not show any decrease during the same time. This again proves the existence of at least two different dynamics: $L_5$ and $L_6$ (the slower one) on the one hand, the FLS on the other. This is consistent with our previous finding of a slower spin-lattice relaxation for $L_5$ and $L_6$ as compared with the FLS.
More insight into these magnetic states dynamics is obtained by studying their EPR signal decrease with increasing temperature, under a 405 nm constant illumination (Figure 2-b). Three different dynamics are observed in the studied temperature range, since the FLS drastically decreases with temperature, while $L_5$ undergoes a moderate decrease and $L_6$ does practically not decrease. At room temperature, no light-induced lines are observed at all. The observed shifts in the resonance field between experiment (a) and (b) (Figure 2) is due to the change in the MW frequency $\nu$, the corresponding $g$-factors remaining constant.

In order to obtain a clear and quantitative comparison between these dynamics, the normalized EPR intensities

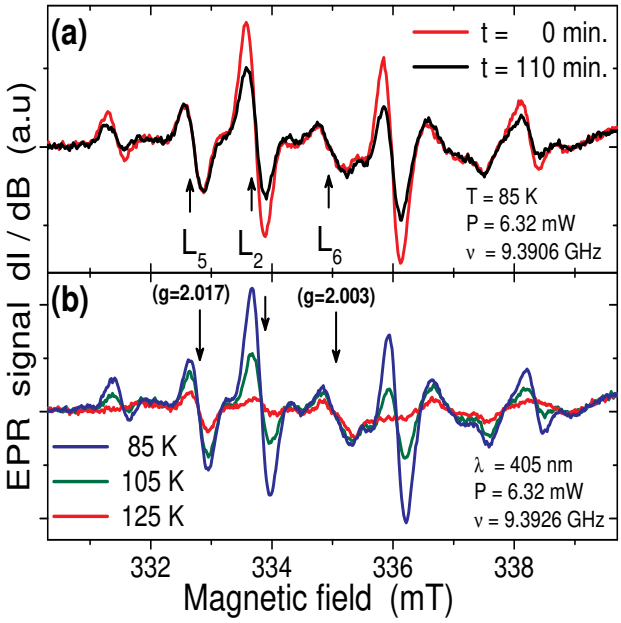


**Figure 2** (color online) (a) Evolution of EPR spectra with time after 405 nm illumination removal (1 scan per spectrum), recorded at $T = 85$ K. (b) Evolution of EPR spectra with increasing temperature under constant illumination at 405 nm (4 scans per spectrum). (a) and (b) recorded 6 months after growth.

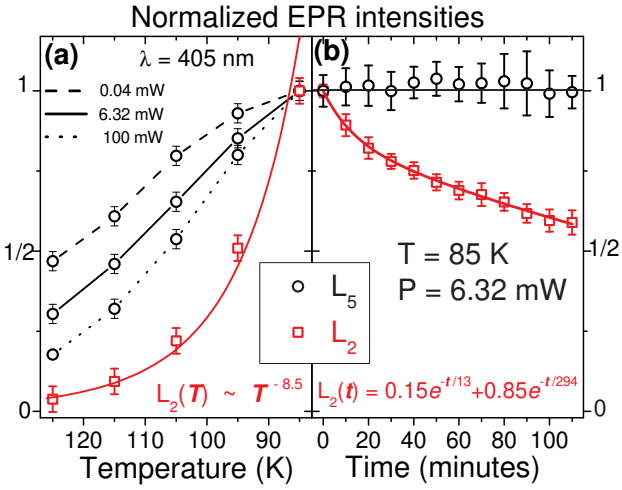


**Figure 3** (color online) Normalized EPR intensity decay of $L_2$ and $L_5$ lines, (a) with increasing temperature under constant illumination (for three MW powers for $L_5$), and (b) with time after illumination removal at $T = 85$ K. Red continuous lines show the fits for the $L_2$ decays, whose equations are displayed in figures.

of $L_2$ and $L_5$ have been plotted as functions of temperature (under constant excitation) and time (after excitation removal) in Figure 3. The evolution of $L_2$ can be considered as representative of the FLS and that of $L_3$ is ignored for simplification.

The fit of the $L_2$ intensity's decay with temperature depicted in Figure 3-a reveals a $T^{-8.5}$ dependence, independent of the MW power (within the error bars). Divergence from this fit logically occurs at lower temperature because an inflexion point must exist: the EPR intensity remains finite as $T \rightarrow 0$. In EPR of ground states, the intensity $I$ decreases with increasing temperature because of the equalization of the resonating-level population, resulting in a Curie law at high temperature ($I \sim T^{-1}$). This is clearly not the case here, where the strong intensity's decay with temperature is most probably due to the depopulating of the excited state *via* high-order processes.
The temperature dependence of the $L_5$ line is different for it depends on the MW power and for it shows the inflexion point (visible by the use of scatter-line plots), indicating an intermediate temperature regime. This temperature dependence has not been fitted so far, since without the exact knowledge of the involved spin-system it does not bring much information.
The intensity's evolution with time of $L_5$ is shown in Figure 3-b, which is simply fitted by a constant function. Besides, the $L_2$ intensity is fitted by a bi-exponential decay, whose equation is denoted in Figure 3-b (time constants 13 min. and 294 min.), indicating the coexistence of two mechanisms contributing to the relaxation of $L_2$, respectively by 15 % and 85 % of the total decay. Regarding the time scale involved in the magnetic resonance relaxation ($10^{-9}$–$10^{-7}$ s), these time constants can be viewed as almost infinite. This suggests a very indirect recombination process, consistently with a spin-forbidden transition of a high spin state. An intermediate $J = 0$ state would then have to be (thermally or otherwise) reached for allowing the electron-hole recombination.

All the presented results prove the existence of at least two different optically-excited localized magnetic states, characterized by quite unusual long life-times. The excitation energy lays in the visible violet region for all of the detected EPR lines, well below the ZnO band gap energy. In terms of both stability with temperature and duration with time, the $L_5$ line appears to be very promising for applications. On the other hand, the FLS is also of great interest for it displays a weak but sizeable anisotropy, together with a probable high effective-spin $J = 2$. The coexistence of the FLS and the additional light-induced lines $L_5$ and $L_6$ points to a rather complex situation in which charged point defects, fictious surface charges, bi-exciton coupling or surface traps could be involved. Confinement effects would also be likely to favour the stabilization of these magnetic states, via the space quantization of the photo-generated charges. In any case, the NPs surface certainly plays a crucial role in the appareance of these magnetic states, since they have never been observed in bulk or micro-sized ZnO crystals. The observation of this new magneto-optical effect is moreover complicated by the necessary long relaxation time of the NPs after growth, which probably explains the absence of previous reports[15]. Indeed, $O_2$ molecules are known to passivate the ZnO surface and to act as hole surface traps. Under UV-vis illumination, the photogenerated holes neutralize the oxygen ions leading to $O_2$ desorption: the remaining photogenerated electrons then increase the n-type conductivity[17, 18]. The persistent photocurrent (after illumination removal) has decay time of the order of several hours[18, 19], suggesting that a similar or analogous phenomenon is presently observed. The observed very long life-times are compatible with some spin-forbidden transitions, as would be expected for the quintet ($J = 2$) or triplet ($J = 1$) states of some dark bound excitons[20].
Although complementary experiments will be required in order to draw a complete picture of this new magneto-optical effect, a demonstration of its potentiality is given in this letter. The observed optically-excited and long-standing magnetic states are very promising for future applications in the field of information storage and processing.

**Acknowledgements** Adrien Savoyant acknowledges Sylvain Bertaina, Olivier Pilone and André Ghorayeb for fruitful discussion, technical help and relecture, respectively.

## References

[1] Al.-L. Éfros and A.-L. Éfros, Sov. Phys. Semicond. **16** 772 (1982).
[2] A. I. Ekimov, Al. L. Efros, A. A. Onushchenko, Solid State Commun. **56** 921 (1985).
[3] M. Rajalakshmi, A. K. Arora, B. S. Bendre, and S. Mahamuni, J. Appl. Phys. **87** 2445 (2000).
[4] V.-I. Korepanov, S.-Y. Chan, H.-C. Hsu, H.-o, and Hamaguchi, Heliyon **5** e01222 (2019).
[5] K. Mabhouti, M. Karamirad, P. Norouzzadeh, M. M. Golzan, and R. Naderali, J. Electron. Mater. (2020).
[6] S. Baruah, S.-S. Sinha, B. Ghosh, S.-K. Pal, A.-K. Raychaudhuri, and J. Dutta, J. Appl. Phys **105** 074308 (2009).
[7] P. Jakes and E. Erdem, Phys. Status solidi RRL **5** 56 (2011).
[8] Al. L. Efros and A. V. Rodina, Solid State Commun. **72** 645 (1989).
[9] Y. Gu, I.-L. Kuskovsky, M. Yin, S. O'Brian, and G.-F. Neumark, Appl. Phys. Lett. **85** 3833 (2004).
[10] O. Dulub, U. Diebold, and G. Kresse, Phys. Rev. Lett. **90** 016102 (2003).
[11] A. Savoyant, M. Rollo, M. Texier, R. E. Adam, S. Bernardini, O. Pilone, O. Margeat, O. Nur, M. Willander, and S. Bertaina, Nanotechnology **31**, 095707 (2020).
[12] N. T. Thang and G. Fishman, Phys. Rev. B **31** 2404 (1985).
[13] Y. K. Frodason, K. M. Johansen, T. S. Bjørheim, , and B. J. Svensson, Phys. Rev. B **95** 094105 (2017).
[14] A. K. Diallo, M. Gaceur, N. Berton, O. Margeat, J. Ackermann, and C. Videlot-Ackermann, Superlattices Microstruct. **58** 144 (2013).
[15] E. Erdem, J. Alloys Compd. **605** 34 (2014).
[16] A. Savoyant, H. Alnoor, S. Bertaina, O. Nur, and M. Willander, Nanotechnology **28** 035705 (2017).

[17] C. Soci, A. Zhang, B. Xiang, S. A. Dayeh, D. P. R. Aplin, J. Park, X. Y. Bao, Y. H. Lo, and D. Wang, Nano Lett. **7** 1003 (2007).
[18] J. Bao, I. Shalish, Z. Su, R. Gurwitz, F. Capasso, X. Wang, and Z. Ren, Nanoscale Res. Lett. **6** 404 (2011).
[19] L. Lu, X. Jiang, H. Peng, D. Zeng, and C. Xie, RSC Adv. **8** 16455 (2018).
[20] E. Poem, Y. Kodriano, C. Tradonsky, N. H. Linder, B. D. Gerardot, P. M. Petroff, and D. Gershoni, Nat. Phys **6** 993 (2011).